

CHEMISTRY

A European Journal

A Journal of



Accepted Article

Title: Synthesis of EU-1/ZSM-48 Co-crystalline Zeolite by High Silica EU-1 Seeds: Tailoring Phase Proportions and Promoting Long Crystalline Phase Stability

Authors: Yafei Zhang, Yasheng Liu, Liyuan Sun, Luoming Zhang, Jun Xu, Feng Deng, and Yanjun Gong

This manuscript has been accepted after peer review and appears as an Accepted Article online prior to editing, proofing, and formal publication of the final Version of Record (VoR). This work is currently citable by using the Digital Object Identifier (DOI) given below. The VoR will be published online in Early View as soon as possible and may be different to this Accepted Article as a result of editing. Readers should obtain the VoR from the journal website shown below when it is published to ensure accuracy of information. The authors are responsible for the content of this Accepted Article.

To be cited as: *Chem. Eur. J.* 10.1002/chem.201705805

Link to VoR: <http://dx.doi.org/10.1002/chem.201705805>

Supported by
ACES

WILEY-VCH

FULL PAPER

Synthesis of EU-1/ZSM-48 Co-crystalline Zeolite by High Silica EU-1 Seeds: Tailoring Phase Proportions and Promoting Long Crystalline Phase Stability

Yafei Zhang,^[a] Yasheng Liu,^[a] Liyuan Sun,^[a] Luoming Zhang,^[a] Jun Xu,^[b] Feng Deng^[b] and Yanjun Gong*^[a]

Abstract: A facile, specific seeds-assisted strategy for the synthesis of EU-1/ZSM-48 co-crystalline zeolite in the presence of hexamethonium ions (HM²⁺) has been developed. EU-1/ZSM-48 co-crystalline zeolites with various phase proportions, with EU-1 in the range of 25 wt%-86 wt%, were obtained by adding high silica EU-1 seeds (SiO₂/Al₂O₃ ratio of 300) and adjusting the synthesis parameters. Not only the phase proportions of EU-1/ZSM-48 co-crystalline zeolite can be controlled but also the stability period for co-crystallization of the two phases can be extended through varying the amount of EU-1 seeds and the HM²⁺ template. Moreover, with the increase of EU-1 proportion in the EU-1/ZSM-48 co-crystalline, the framework SiO₂/Al₂O₃ ratios of EU-1 phase promotes steadily, pointing to an ever-changing synthesis phase area during the competitive growth of the two phases. Major differences in acidity and textural properties of the EU-1/ZSM-48 co-crystalline zeolites were found with varying phase proportions, due to their distinct topological structures and crystal morphology and asymmetry between the EU-1 and ZSM-48 phases. For instance, EU-1/ZSM-48 zeolite containing 75 wt% of EU-1 (Coz-75) possesses specific acidity and mesoporous characteristics, showing an excellent catalytic activity and stability in n-hexane cracking reaction. Compared to EU-1, ZSM-48 and a mixed one (Mix-75), Coz-75 resulted in the highest hexane conversion and yields of light olefins, with a propylene yield, in particular, up to 38.3 wt%, which is 6.3 percentage point higher than that of Mix-75 sample.

Introduction

Zeolites are widely used in oil refining, fine chemicals production, and adsorption/separation fields due to their diverse topological structures and adjustable acidities.^[1]

Zeolites are metastable materials and in most cases, a perfect crystalline phase could be obtained only when the synthesis parameters are precisely tuned. It is a common phenomenon that the majority of zeolite crystallization conditions often result in the formation of materials with several different topological phases, which can be treated as zeolite-zeolite composite.^[2] Zeolite-zeolite composite is usually constructed by two-phase intergrowth (epitaxial and polytypism) and/or co-crystalline (or co-growth) during the crystallization process.^[3] Hence, the composite with different zeolitic phases not only possesses advantages of the individual zeolite structure, but also displays specific pore structure and acid property, which leads to unique synergistic performance in various catalytic reactions.^[2a,2b] Accordingly, enormous efforts have been devoted to the synthesis of new intergrowth or co-crystalline zeolites and to the further development of their potential applications.^[4]

The two zeolites that can form an intergrowth zeolite should be structurally related or have similar planar building units and elemental composition. These similar composition units could induce stacking in different sequences or oriented overgrowth upon different phases.^[5] MFI/MEL zeolite, for example, is one of the typical intergrowth zeolites and has drawn great attention both for academic research and industrial application.^[6] Some intergrowth zeolites may provide the opportunity for the construction of multidimensional nanospacial network, such as zeolite beta,^[7] STF/SFF,^[8] CHA/AEI,^[9] NON/EUO/NES,^[10] MTT/TON,^[11] and ETS-10/ETS-4.^[12]

In contrast, the co-crystalline zeolites are formed without necessarily requiring a structural similarity between the two crystal units. Co-crystalline zeolites can be structurally fabricated by diversified crystal forms according to the actual design arrangement.^[13] The synthesis of co-crystalline zeolites can usually adopt a simple one-pot synthetic strategy mainly by employing dual templates or a single template with seed-assisted system.^[4,13d] For instance, MCM-49/ZSM-35 co-crystalline zeolite was synthesized in the mixed amines system composed of hexamethyleneimine (HMI) and cyclohexylamine (CHA), with HMI acting as the template for the formation MCM-49 phase, and CHA directing the structure of ZSM-35 phase in MCM-49/ZSM-35 composites was adjusted by the molar ratio of HMI/CHA.^[4] A noteworthy aspect of the seeded approach is that one of the crystal phases in the co-crystalline zeolite could be induced by organic template, while the other phase could be generated with the assist of seeds.^[13d]

[a] Dr. Y. Zhang, Y. Liu, L. Sun, L. Zhang, Prof. Y. Gong*
State Key Laboratory of Heavy Oil Processing and the Key
Laboratory of Catalysis of CNPC,
China University of Petroleum-Beijing, 102249, Beijing, China
E-mail: gongyj@cup.edu.cn

[b] Prof. J. Xu, Prof. F. Deng
State Key Laboratory of Magnetic Resonance and Atomic and
Molecular Physics, Wuhan Centre for Magnetic Resonance,
Wuhan Institute of Physics and Mathematics, Chinese Academy of
Sciences, 430071, Wuhan,

Supporting information for this article is given via a link at the end
of the document

FULL PAPER

The excellent results on co-crystalline zeolites were obtained in many catalytic reactions, including light paraffin cracking, oil catalytic cracking, and aryl alkylation and so on, due to their structurally synergic effect.^[14] The SAPO-11/H β co-crystalline zeolite gave rise to higher selectivity both for propylene and ethylene in the cracking reaction of 2-butene when compared to the system utilizing a mechanically mixed zeolite sample. This was mainly attributed to the increased density of Brønsted acid sites and higher ratio of Brønsted/Lewis acid sites due to the presence of strong chemical interaction between SAPO-11 and H β phases in the co-crystalline zeolites.^[13d] ZSM-5/Y co-crystalline zeolites exhibited an increase in the production of gasoline and the decrease in the yield of light cycle oil (LCO) and coke in the heavy oil cracking reaction, due to the unique structural complement within the ZSM-5 and Y phase.^[15] Most recently, EU-1/ZSM-48 composite exhibited high yield of i-hexadecane compared to mechanical mixtures of zeolites in the hexadecane hydroisomerization reaction.^[24]

ZSM-48 (*MRE) is a high-silica zeolite with a one-dimensional 10-ring pore system and crystal face (100). Due to the highly-disordered framework, the catalytic performance of ZSM-48 zeolite can be readily adjusted by controlling the disorder degree from different synthesis processes. It was found that ZSM-48 has higher propylene selectivity than the conventional ZSM-5 in the catalytic cracking reaction of C4-olefins.^[16]

EU-1 zeolite (EUO) has a one-dimensional 10-ring pore system with crystal face (100), but is periodically interrupted by alternating "side-pockets" circumscribed by 12-ring along with crystal face (001).^[17] Since the original report of EU-1 zeolite in 1985 by Casci et al.,^[18] much effort has been devoted to the optimization of its primary structural properties, by a variety of methods, such as variation of the crystal morphology/size, widening of the range of framework Si/Al ratio, and the introduction of mesopores into the crystals. In the early report, the synthesis of pure EU-1 phase in hexamethonium ions (HM) medium was strongly confined to the gel compositions and crystallization conditions. Pure EU-1 was only obtained when the SiO₂/Al₂O₃ ratio in the initial gel was less than 120. An increased SiO₂/Al₂O₃ ratio would lead to the formation of mixed phases of EU-1 and ZSM-48 or even pure ZSM-48.^[18] Meanwhile, alumina rich EU-1 could be readily prepared in an HM rich system, whereas ZSM-48 zeolite was favored with low ratios of OH/SiO₂ and OH/HM (between 2.5 and 5).^[19] It was later reported that all-silica EU-1 zeolite was synthesized by employing the strategy of dry-gel conversion,^[20] indicating that the extremely high HM concentration, due to a small amount of water in the gel, was conducive to inhibiting the ZSM-48 phase. In our previous work, by using Al-rich EU-1 seeds, pure EU-1 zeolites with a wide range of SiO₂/Al₂O₃ ratios (55-1500) has been successfully prepared in the optimized HM system. The result indicates that Al-rich EU-1 seeds (SiO₂/Al₂O₃ ratio of ca.55) can reduce the activation energy for EU-1 nucleation, and hence inhibits the crystal transformation from EU-1 into ZSM-48 during the long crystallization process, and finally leads to the formation of high-silica EU-1 zeolite.^[21]

There has been a growing interest in replacing the current steam cracking process of naphtha to produce light olefins by catalytic ones. A major challenge is the exploration

of highly effective catalysts. Recently, EU-1 zeolites with SiO₂/Al₂O₃ ratios ranging from 55 to 300 were evaluated systemically in the n-hexane cracking reaction.^[22] We have observed that high silica EU-1 (SiO₂/Al₂O₃ ratio of ca. 300, EU-1-300) exhibited a high propylene selectivity of up to ~35%, an increase of 9.6 percentage points compared to ZSM-5-300. Moreover, EU-1 zeolites would produce the low aromatic hydrocarbons, which could be attributed to the more confined channel system (0.41 × 0.58 nm). Meanwhile, ZSM-48-300 was also shown to exhibit high propylene selectivity and low aromatics compared to the best alternative ZSM-5.^[22] In addition, EU-1 zeolites have tremendous potential for applications in the isomerization of aromatics and the conversion of methanol to hydrocarbons.^[23]

Therefore, new approaches to zeolitic composite with EU-1 and ZSM-48 structures, ideally in a one-pot synthesis, have become highly desirable and attracted great academic and industrial interests. Due to the possibility to induce distortion of zeolitic microstructure, the composite zeolite properties, including its acidity and texture property, can be finely tuned during the competitive co-growth process and may eventually exert excellent catalytic activity. Still, there exist many challenges in the specific design of the co-crystalline structure and in the control of phase proportion, particularly it applies to a specific reaction. On the one hand, a slight change in the synthesis conditions would result in the transformation between the two zeolites, leading to the uncertainty of phase proportion of the co-crystalline. Thus, the co-crystalline zeolites cannot be tuned and the physicochemical properties are hardly predictable. On the other hand, it is quite difficult to retain a long period of crystallization stability for the co-crystalline zeolite, due to the synthetic phase area and phase composition for the individual zeolites are dynamically changing during the co-growing process.

Herein we wish to report a facile strategy for controllable synthesis of EU-1/ZSM-48 co-crystalline zeolite by employing specific EU-1 seeds in the presence of a HM single-template. As a result, EU-1/ZSM-48 co-crystalline zeolites with series of phase proportions were obtained with a wide range of EU-1 phase proportions (25 wt%-86 wt%). The specific high silica EU-1 seeds played a pivotal role in controlling the phase proportion, also providing a long period of stability of the resulting EU-1/ZSM-48 co-crystalline zeolite. Research firstly provides the new insight into the way of EU-1 framework SiO₂/Al₂O₃ ratios behave as varying the phase proportion in the EU-1/ZSM-48. The crystallization process regulating the phase proportion of the EU-1/ZSM-48 are proposed. Its catalytic performance was also evaluated in catalytic n-hexane cracking reaction.

Results and Discussion

Effect of seeds on the crystallization process of EU-1/ZSM-48 co-crystalline zeolite: As our reported, Al-rich EU-1 seeds (i.e. SiO₂/Al₂O₃ ratio of 55) was required for the synthesis of high silica EU-1 zeolite (SiO₂/Al₂O₃ ratio > 120), because it could facilitate the nucleation/growth of EU-1 and inhibit the formation

FULL PAPER

of ZSM-48 phase.^[21] Instead, an attempt to choose high silica seeds to examine the influence on the co-growth behavior of EU-1 and ZSM-48 phases is very meaningful. Figure 1 shows the relationship between crystalline phase content and crystallization time at 453 K, where 2.5 wt% of EU-1-300, ZSM-48-300 and Mix-55 were used as seeds, respectively (300 refers to the SiO₂/Al₂O₃ ratio of the initial prepared gels for EU-1 and ZSM-48 and 55 is the EU-1 proportion in the mechanical mixture of EU-1-300 and ZSM-48-300. The sum of crystalline phase content of EU-1 and ZSM-48 approximates the content of EU-1/ZSM-48).

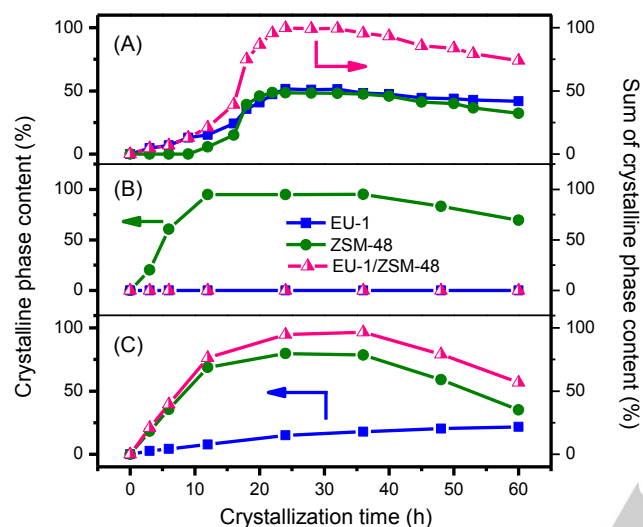


Figure 1. The variation of crystalline phase content with crystallization time at 453 K with the different seeds (A) EU-1-300 (B) ZSM-48-300 and (C) Mix-55.

The EU-1/ZSM-48 co-crystalline zeolites are obtained only in the presence of EU-1-300 (Figure 1A) or the Mix-55 seeds (Figure 1C), while ZSM-48-300 as seeds leads to the formation of well-crystallized pure ZSM-48 zeolite (Figure 1B). Note that if the Mix-55 is used as seeds, both EU-1 and ZSM-48 phases appear simultaneously and increase with crystallization time, but the rate of increase upon ZSM-48 is much more remarkable at the initial stage. In this case, the variation trend of ZSM-48 content has a perfect parabola, while the content of EU-1 rises gradually, which suggests the EU-1/ZSM-48 co-crystalline zeolite with large proportion of ZSM-48 is formed and the phase proportions are ever-changing with time. As can be observed in the EU-1-300 seed system, the EU-1 crystals firstly appear and the ZSM-48 phase begins to emerge after 10 h, then both phases co-grow in a nearly consistent rate. These results indicate that EU-1-300 seeds not only facilitate the growth of EU-1/ZSM-48 co-crystalline zeolite, but also provide a relatively long period of crystallization stability (keeping invariable phase proportion from 20 h to 36 h) during the crystallization process. XRD patterns of the samples obtained at different crystallization time with EU-1-300 seeds were displayed in Figure S2. The co-crystalline zeolite with expected phase proportion would have more competitive advantage over others because the long period of crystallization stability is necessary for controllable and large-scale preparation under an industrial condition.

Figure 2 shows XRD patterns of EU-1, ZSM-48, EU-1/ZSM-48 co-crystalline and the mixed one. All samples have well-

crystallized structures. The EU-1/ZSM-48 co-crystalline and their mechanical mixture samples exhibit the characteristic diffraction peaks of both EU-1 and ZSM-48 phases, and almost similar to each other.

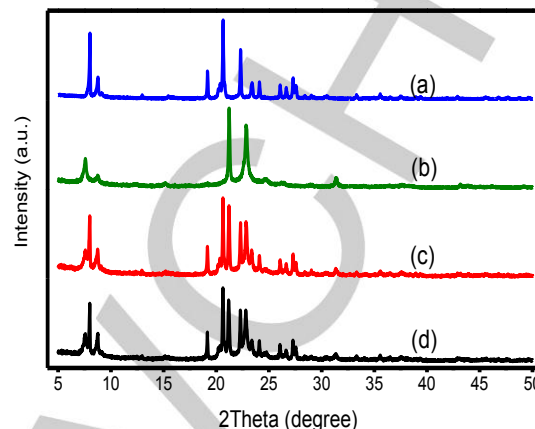


Figure 2. XRD patterns of (a) EU-1 (b) ZSM-48 (c) EU-1/ZSM-48 (d) Mechanical mixture.

SEM images (Figure 3) reveal that EU-1 zeolite presents petal-like crystal (Figure 3a) while ZSM-48 possesses strips morphology with thin fibres binding together (Figure 3b). However, ZSM-48 phase in EU-1/ZSM-48 co-crystalline zeolite changes into stacks of small crystals and embeds into the petal-like EU-1 crystals while the mechanical mixture sample shows only the discrete mixture of the two kinds of crystals. These results well demonstrate the formation of EU-1/ZSM-48 co-crystalline zeolites during the crystallization process.

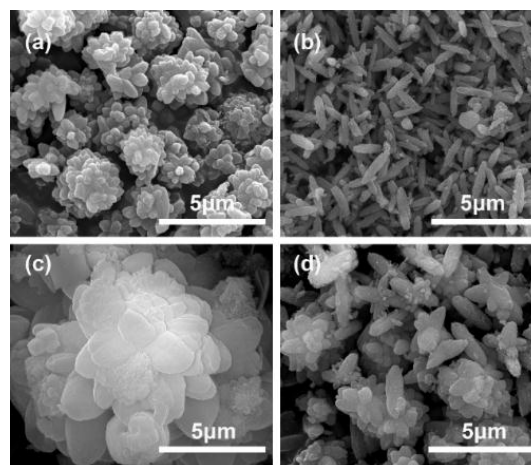


Figure 3. SEM images of (a) EU-1 (b) ZSM-48 (c) EU-1/ZSM-48 (d) Mechanical mixture.

Tuning the crystal phase proportions of EU-1/ZSM-48 co-crystalline zeolites: Using EU-1-300 as seeds in the gel composition of SiO₂-1/300Al₂O₃-0.12Na₂O-0.08HMBBr₂·12H₂O, the effect by adding seed on crystal phase proportion was

FULL PAPER

investigated systematically. Figure 4 illustrates the seed content as a function of EU-1 phase proportion in EU-1/ZSM-48 co-crystalline zeolites. In the absence of EU-1 seed in the initial gel, only ZSM-48 phase was detected in the resulting sample due to the high silica mixture gel, which is consistent with previous work.^[21] After addition of EU-1-300 seeds, with the seeds accounting for 1.5 wt% to 6.0 wt% of SiO₂ in the initial gel, the mass fraction of EU-1 phase in co-crystalline zeolite increases from 40% to 80%. When the seed content reaches to 10.0 wt%, the proportion of EU-1 phase in EU-1/ZSM-48 co-crystalline zeolite goes up to 86%, and it cannot increase further with the seeds content. It is deduced that the proportion of EU-1 phase in the resulting co-crystalline zeolites may also related to other factors.

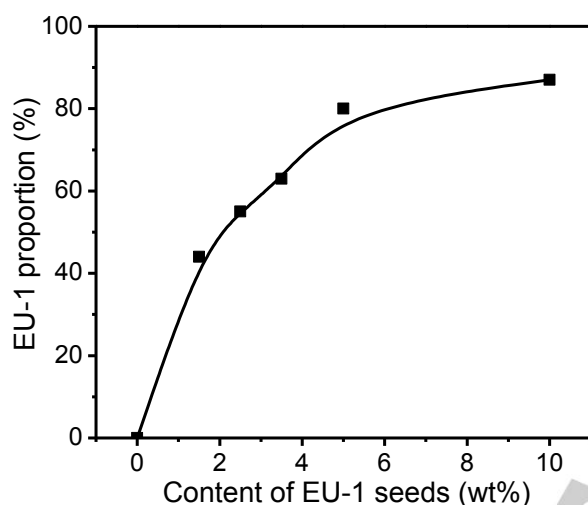


Figure 4. The influence of EU-1 seed content on the proportions of EU-1 phase in the co-crystalline samples.

As known, the template concentration and alkalinity in the initial gel are key factors for the nucleation and crystallization of each zeolite, which also present strong influence on the formation of co-crystalline zeolite.^[25] Table 1 shows the synthesis parameters and corresponding proportion of EU-1 phase in the co-crystalline zeolite. At the same Na₂O/SiO₂ ratio and 2.5 wt% EU-1-300 seeds, the proportion of EU-1 phase remarkably increases with the HM/SiO₂ ratio, which is in perfect accordance with the result that HM rich system favors the synthesis of EU-1 phase.^[21] The length of HM ion is around 14.5 Å, so it can be accommodated in a perpendicular position to the a-axis between the channel and a side-pocket in the framework of EU-1 zeolite, but only can be filled in the channel of ZSM-48 zeolite.^[19] As a result, HM accommodation is about 4 per unit cell for EU-1 zeolite and only 1 per unit cell for ZSM-48. Thus, there are more HM ions required to stabilize the EU-1 zeolite negative [Si-O-Al] framework compared with ZSM-48 zeolite. Herein, EU-1 proportion varies from 25% to 86% with the HM/SiO₂ ratio ranges from 0.04 to 0.15.

The influence of alkalinity is also exhibited in Table 1. When Na₂O/SiO₂ ratio is 0.06, EU-1/ZSM-48 mixing with amorphous materials is obtained, showing a very low relative crystallinity (Sample 6). Increasing Na₂O/SiO₂ ratio from 0.06 to 0.16, the crystallinity of EU-1/ZSM-48 co-crystalline zeolite increases gradually, while EU-1 proportion in co-crystalline zeolites retains

50%-55% (Sample 7, 3, 8). Therefore, HM ions mainly direct the structure of EU-1 phase, while the suitable alkalinity (Na₂O/SiO₂ ratio) could improve the crystallinity, and it hardly impacts the EU-1 phase proportion. Interestingly, when using high-silica EU-1-300 as seeds in the high-silica gel with SiO₂/Al₂O₃ ratio of 300 and Na₂O/SiO₂ ratio of 0.12, EU-1/ZSM-48 co-crystalline zeolite was steadily produced. Instead, adding the Al-rich seeds (EU-1-55), only EU-1 phase was produced without formation of ZSM-48.^[21] This suggest Al content in EU-1 seeds could play a crucial role in the balance of formation of EU-1 and ZSM-48 crystalline phase during the crystallization process.

Table 1. Typical products with various EU-1 phase proportions obtained with different concentrations of HM and alkalinity.^[a]

| Sample | Initial gel composition | | Products | |
|--------|-------------------------|------------------------------------|-------------------------|--------------------|
| | HM/SiO ₂ | Na ₂ O/SiO ₂ | Crystalline phases | Proportion of EU-1 |
| 1 | 0.04 | 0.12 | EU-1/ZSM-48 | 25 |
| 2 | 0.06 | 0.12 | EU-1/ZSM-48 | 43 |
| 3 | 0.08 | 0.12 | EU-1/ZSM-48 | 54 |
| 4 | 0.12 | 0.12 | EU-1/ZSM-48 | 75 |
| 5 | 0.15 | 0.12 | EU-1/ZSM-48 | 86 |
| 6 | 0.08 | 0.06 | Amorphous + EU-1/ZSM-48 | — |
| 7 | 0.08 | 0.08 | EU-1/ZSM-48 | 50 |
| 8 | 0.08 | 0.16 | EU-1/ZSM-48 | 55 |

[a] Initial gel composition: SiO₂ - 1/300 Al₂O₃ - x HMBR₂ - y Na₂O - 12H₂O with 2.5 wt% EU-1-300 seeds at 453 K for 36 h, where x varies from 0.04-0.15 and y is from 0.06 to 0.16.

With the same gel composition SiO₂-1/300 Al₂O₃-0.12 Na₂O-0.08 HMBR₂-12 H₂O and 2.5 wt% of EU-1-300 seeds, the relationship between crystalline phase content and crystallization time at 433 K and 453 K are shown in Figure 5. An elevated temperature pronouncedly improves the nucleation, growth and the content of EU-1/ZSM-48 zeolite. At temperature of 433 K, it takes nearly 60 h for completing nucleation and growth of zeolites while it is only 24 h at 453 K. Note that the crystallization period when the well-crystallized products exhibit a stable phase state is called the crystallization stability period. At low temperature (433 K), the resulting co-crystalline has a longer stable period of 50 h and it has ca. 18 h at high temperature of 453 K. Based on the normalized crystallinity of EU-1/ZSM-48 co-crystalline during the stability period, the individual crystallinity of EU-1 and ZSM-48 zeolites at 433 K are about 40% and 35%, respectively, while those are about 51% and 48%, respectively at 453 K. It is notable that the proportion of EU-1 phase in EU-1/ZSM-48 co-crystalline maintains at constant value (about 52-54%) under the two crystallization temperatures. Meticulously examining the curves at 433 K and 453 K, EU-1 is preferential nucleation and growth, while ZSM-48 phase appears after 20 h and 10 h, respectively. The result implies that the both phases have the similar co-growth mechanisms under the two crystallization temperatures, but their growth rate are different.

FULL PAPER

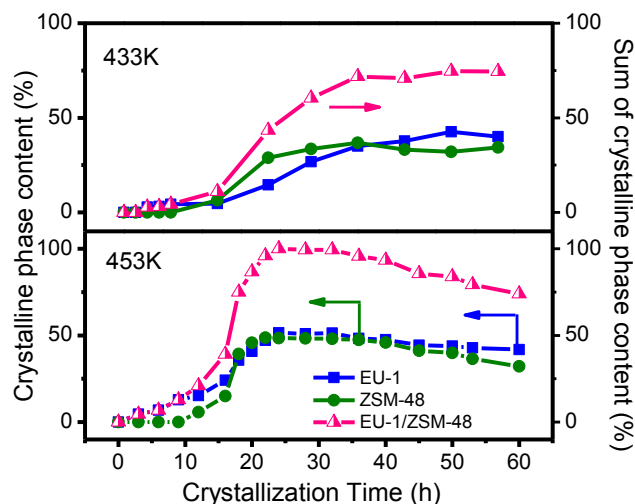


Figure 5. The relationship between crystalline phase content and crystallization time at 433 K and 453 K.

The structural properties of EU-1/ZSM-48 co-crystalline zeolites:

Figure 6 presents the N_2 adsorption/desorption isotherms of the samples. For single EU-1, ZSM-48 and Mix-75, the isotherms exhibit typical type-I curve, indicating their microporous characteristics. Among the samples, Coz-54 and Coz-75 (the co-crystalline zeolites with EU-1 proportions of 54 and 75) exhibit the similar type-IV isotherms with type H3 hysteresis loop, while Coz-86 presents the typical type-I isotherm similar to that of pure EU-1 zeolite. Moreover, there is difference in the H3 hysteresis loops between Coz-54 and Coz-75, particularly the desorption branch at relative pressure P/P_0 of 0.45-0.50. Such isotherms without levelling off at relative pressure close to the saturation vapor pressure indicate the material has slit-like pores from the aggregates of plate-like particles.^[26] For Coz-75, very different from Mix-75, presents a representative modified type-IV isotherms, with a big hysteresis loop corresponding to capillary condensation at $P/P_0=0.45-0.99$. It suggests that the irregular mesoporosity may arise from the voids or defects between co-crystals, and increase the pore volume of the co-crystalline zeolite.^[27] The uneven pore distribution of EU-1/ZSM-48 co-crystalline zeolite changes gradually as increasing the proportion of EU-1 phase as can be observed in Figure S3.

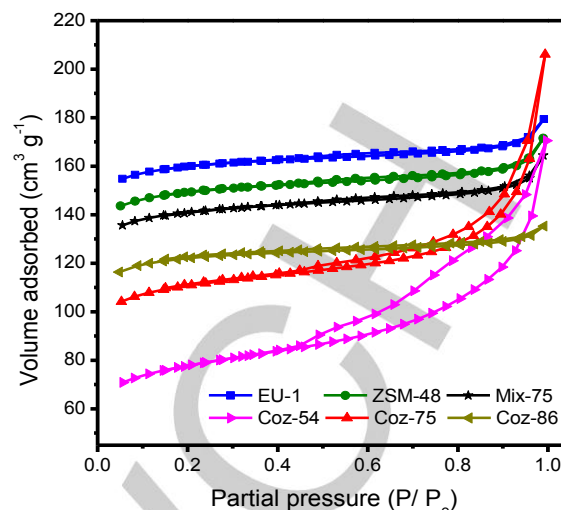


Figure 6. N_2 adsorption/desorption isotherms of the samples. Putting in $20 cm^3 g^{-1}$ offset for the adjacent isotherms up on Y-axis.

Table 2. Texture properties of different zeolite samples.

| Sample | $S_{BET}^{[a]}$ ($m^2 g^{-1}$) | $S_{micro}^{[b]}$ ($m^2 g^{-1}$) | $S_{ext}^{[b]}$ ($m^2 g^{-1}$) | $V_{total}^{[c]}$ ($cm^3 g^{-1}$) | $V_{micro}^{[b]}$ ($cm^3 g^{-1}$) | V_{meso} ($cm^3 g^{-1}$) |
|--------|-------------------------------------|---------------------------------------|-------------------------------------|--|--|---------------------------------|
| EU-1 | 356.1 | 301.5 | 54.6 | 0.20 | 0.15 | 0.05 |
| ZSM-48 | 355.3 | 297.1 | 58.2 | 0.20 | 0.14 | 0.06 |
| Mix-75 | 360.1 | 301.5 | 58.6 | 0.21 | 0.15 | 0.06 |
| Coz-54 | 257.2 | 170.0 | 87.2 | 0.26 | 0.08 | 0.18 |
| Coz-75 | 329.5 | 255.5 | 74.0 | 0.30 | 0.12 | 0.18 |
| Coz-86 | 332.1 | 281.0 | 51.1 | 0.18 | 0.14 | 0.04 |

[a] S_{BET} (BET surface area) obtained from the adsorption isotherm. [b] S_{micro} (micropore area), S_{ext} (external surface area) and V_{micro} (micropore volume) calculated using t-plot method. [c] V_{total} (total pore volume) obtained at $P/P_0=0.99$.

FULL PAPER

Figure 7 shows the acidities of the samples measured by NH_3 -TPD. All of the profiles denote two desorption peaks in the temperature region of 350-550 (Peak l) and 550-850 K (Peak h), which are attributed to the NH_3 desorbed from weak and strong acidic sites, respectively. The acid amount and acid strength by the integrated areas and peak temperatures are listed in Table S7.^[22] Compared to EU-1, ZSM-48 and Mix-75, Coz-75 exhibits remarkably more acid amount, while the acid strength, especially the strong acid is also higher than others. The enhanced acid property of the co-crystalline zeolite mainly ascribes to the crystal defect arising from the symbiotic process and the synergetic effect of acid sites from the two zeolitic phases. The co-crystalline zeolites with different EU-1 proportion, as seen in Fig 7B, display similar acid strength. It suggests that the as-prepared Coz samples by one-pot method may have the close framework Al content due to the same $\text{SiO}_2/\text{Al}_2\text{O}_3$ ratio in synthesis gel. The acid amount of Coz-75 is slightly larger than other two Coz samples.

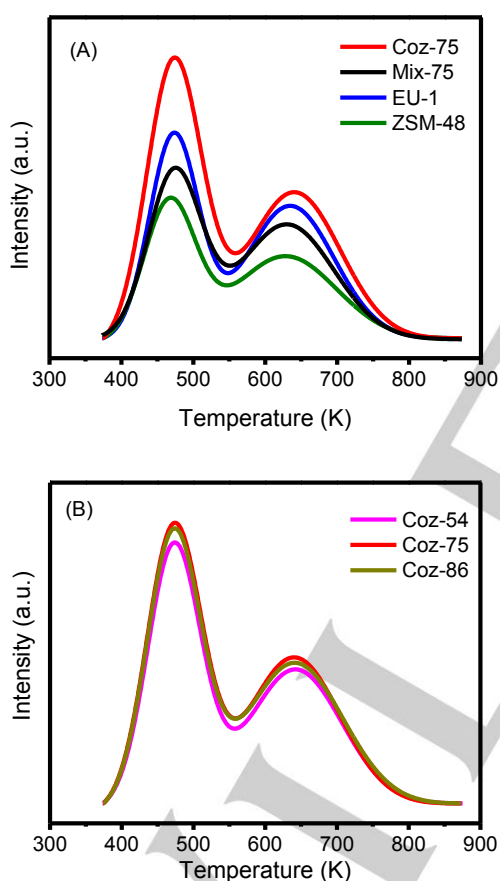


Figure 7. NH_3 -TPD profiles of correlative samples.

Since the acidity of zeolite is strongly dependent on the aluminum site and its coordination environment with framework silica,^[28] The ^{27}Al MAS NMR and ^{29}Si MAS NMR spectra of the relevant samples were determined as shown in Figure 8. The ^{27}Al MAS NMR (Figure 8A) spectra demonstrate only a sharp signal at 52 ppm on each sample, which is assigned to tetrahedral coordinated framework aluminum species. No signal around 0

ppm is found, indicating all the aluminum species are incorporated into the zeolite framework.^[29]

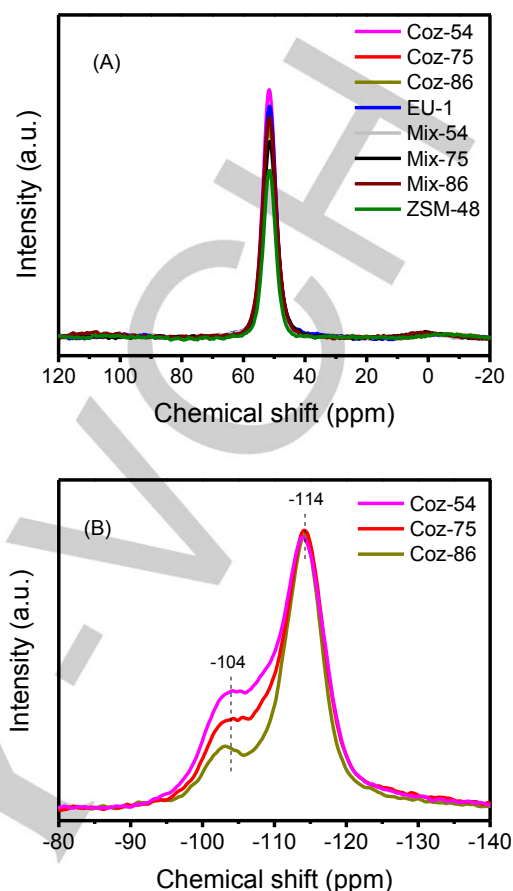


Figure 8. (A) ^{27}Al MAS NMR of the correlative samples and (B) ^{29}Si MAS NMR spectra of Coz-54, Coz-75 and Coz-86 samples.

Figure 8B shows ^{29}Si MAS NMR spectra of Coz-54, Coz-75 and Coz-86 zeolites. The two resonances at -104 and -114 ppm are attributed to the Q^4 species of Si (3Si, 1Al) and Q^4 Si (4Si, 0Al), respectively.^[30] The relative intensity of signal at -104 ppm markedly decreases with EU-1 phase proportion increases from 54% to 86%, while there is almost invariable for the peak at -114 ppm. It could be deduced that number of aluminum atoms incorporated into the framework of EU-1/ZSM-48 co-crystalline zeolites decrease as increasing the EU-1 proportion. In sharp contrast, for pure EU-1, ZSM-48 and their mechanical mixture, both signals at -104 and -114 ppm exhibit an irregular change in intensity, due to the different mixing proportions of the two phases (Figure S4). For zeolites with relatively high $\text{SiO}_2/\text{Al}_2\text{O}_3$ ratio, ^{29}Si MAS NMR has not been used to calculate the framework $\text{SiO}_2/\text{Al}_2\text{O}_3$ ratio precisely.^[31]

FT-IR spectra, as our previous report, could provide the information for the variation of $\text{SiO}_2/\text{Al}_2\text{O}_3$ ratio in EU-1 zeolite.^[21] To identify the content of framework aluminum that incorporated into each crystal phase in the co-crystalline zeolite, FT-IR spectra of the correlative samples are presented in Figure S5. The vibration peaks at 450-470, 540-650, 770-800 and 970-1220 cm^{-1} are assigned to the characteristic bands of EU-1 zeolite.^[32] For all the samples, except the vibrations in the region of 540-650 cm^{-1} , the other three bands have neither nor change in wavenumber

FULL PAPER

and the vibration intensity, which are assigned to the Si-O band, external link symmetric stretch and internal tetrahedral asymmetric stretch, respectively. The band of 540-650 cm^{-1} related to external linkages between the tetrahedral unit is sensitive to the framework structure and the presence of some secondary building unit and building block polyhedra, such as the

double rings and large pore openings.^[32] Therefore, the corresponding region of 500-900 cm^{-1} is amplified (Figure 9). In order to investigate the variation in sample structures of EU-1, ZSM-48 and their co-crystalline and mechanical mixture zeolites with different EU-1 contents.

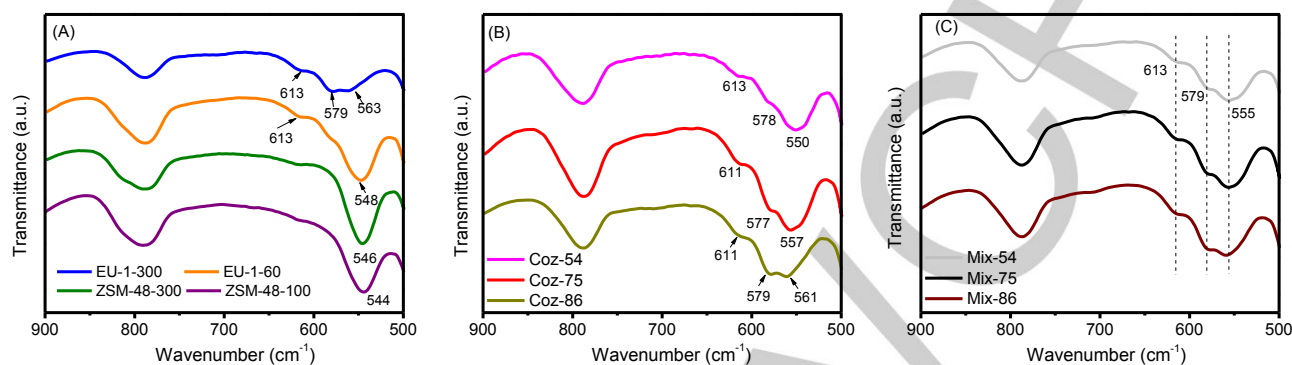


Figure 9. FT-IR spectra of the correlative samples.

As in Figure 9A, two vibrations at 548 and 613 cm^{-1} are observed for EU-1-60, whereas for EU-1-300, an extra strong vibration at 579 cm^{-1} occurs and the band at 548 cm^{-1} shifts to 563 cm^{-1} . Rao reported that there was a strong band at 572 cm^{-1} in high-silica EU-1 zeolite wherein the $\text{SiO}_2/\text{Al}_2\text{O}_3$ ratio higher than 120, using a mixture of benzyldimethylamine (BDMA) and benzyl chloride as the templating agents, and IR absorption bands in this region should be assigned to the vibration of the double rings in high-silica zeolite frameworks.^[32] ZSM-48 presents only one vibration at about 548 cm^{-1} regardless of $\text{SiO}_2/\text{Al}_2\text{O}_3$ ratios. The co-crystalline zeolites and mechanical mixture samples display three vibrations, but the peaks have significant distinctions with the increase of EU-1 contents. For mixture samples (Figure 9C), when the EU-1 proportion increases from 54% to 86%, three vibration bands in the region of 540-650 cm^{-1} remain unchanged (neither the wavenumber nor the intensity). Interestingly, the co-crystalline zeolites, Coz-54, Coz-75 and Coz-86 has the band shift from 550, 557 to 561 cm^{-1} , respectively (Figure 9B) due to the increase of the EU-1 content. Meanwhile, the intensity of shoulder band at 577 cm^{-1} increases gradually with the increase of EU-1 content in co-crystalline zeolites. Moreover, the intensity ratio of the maximum peak at 579 cm^{-1} to 561 cm^{-1} increases largely in Coz-86, which is close to that of EU-1-300. Because of no vibrational peak around 577-579 cm^{-1} for ZSM-48 zeolite, the intensity change in the co-crystalline samples affirmatively is caused by the framework $\text{SiO}_2/\text{Al}_2\text{O}_3$ ratio of EU-1 phase. This result qualitatively demonstrates that $\text{SiO}_2/\text{Al}_2\text{O}_3$ ratio of EU-1 crystal increase with the increase of EU-1 phase proportion in the co-crystalline zeolites.

The unit cell parameters of zeolites could provide a powerful evidence for the variation of framework $\text{SiO}_2/\text{Al}_2\text{O}_3$ ratio due to the shorter length of Si-O band than that of Al-O band.^[21] Thus, the unit cell parameters of the correlative samples were specifically determined from XRD data and shown in Table 3. It is obvious that the unit cell for pure EU-1-60 is larger than that of EU-1-300, and the unit cell volumes are 6271.650 \AA^3 and 6186.802 \AA^3 , respectively. For the co-crystalline zeolites, the unit cell values of a, b, and c for EU-1 phase decrease with the increase of EU-1

proportion, and the cell volumes gradually close to that of pure EU-1-300.

Table 3. The $\text{SiO}_2/\text{Al}_2\text{O}_3$ ratio and unit cell parameters of EU-1 phase in the correlative samples.

| Samples | $\text{SiO}_2/\text{Al}_2\text{O}_3$ ^[a] | Unit cell parameters (\AA) ^[b] | | | $V(\text{\AA}^3)$ |
|----------|---|--|--------|--------|-------------------|
| | | a | b | c | |
| EU-1-60 | — | 13.757 | 22.345 | 20.402 | 6271.650 |
| Coz-54 | 129.86 | 13.729 | 22.249 | 20.317 | 6205.840 |
| Coz-75 | 129.39 | 13.721 | 22.241 | 20.307 | 6197.062 |
| Coz-86 | 131.17 | 13.716 | 22.224 | 20.297 | 6187.177 |
| Mix-54 | — | 13.715 | 22.224 | 20.294 | 6185.655 |
| Mix-75 | — | 13.715 | 22.225 | 20.294 | 6185.933 |
| Mix-86 | — | 13.713 | 22.225 | 20.294 | 6185.031 |
| EU-1-300 | 156.99 | 13.716 | 22.226 | 20.294 | 6186.802 |

[a] Determined by XRF method.

[b] The date of unit cell parameters are calculated by XRD date using the Miller indices of (1,1,4), (2,4,0), (1,3,4), (0,2,5), (0,6,0), and (4,0,0) and the d values they are relevant to.

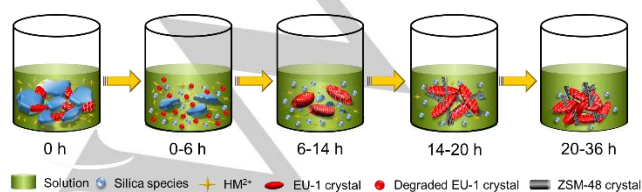
The significant decrease in the unit cell volume suggests that the $\text{SiO}_2/\text{Al}_2\text{O}_3$ ratio of EU-1 crystal phase in co-crystalline zeolites increases with the EU-1 proportion, which is good agreement with the results from FT-IR experiments. Obviously, the values of unit cell parameters of EU-1 crystals for the mechanical mixtures are irrelevant to the content of EU-1 phase. The $\text{SiO}_2/\text{Al}_2\text{O}_3$ ratios determined from XRF present similar values of about 130 for Coz-54, Coz-75 and Coz-86 samples. These changes in co-crystalline framework should be ascribed to the two phases competitive co-growth in the synthesis of EU-1/ZSM-48 co-crystalline zeolites. It has been confirmed that ZSM-48 was favourably formed with high $\text{SiO}_2/\text{Al}_2\text{O}_3$ ratio mixing gel, thus as the co-growth

FULL PAPER

process of EU-1/ZSM-48, higher EU-1 content would make the decrease of $\text{SiO}_2/\text{Al}_2\text{O}_3$ ratio in the reaction gel, leading to the decrease of proportion of ZSM-48 in the resulting EU-1/ZSM-48 zeolite. As a result, no crystal transformation from EU-1 to ZSM-48 is detected during the co-growth process, which leads to the long period of two phase co-crystallization stability.

Primary crystallization process of EU-1/ZSM-48 co-crystalline zeolites:

The insights into the EU-1/ZSM-48 co-crystallization is primarily described in Scheme 1. XRD patterns in Figure S2 show the solid products with crystallization time. Firstly, the synthesis gel is prepared with large silica particles and EU-1-300 seeds with initial molar composition of $\text{SiO}_2\text{-}1/300 \text{ Al}_2\text{O}_3\text{-}0.12 \text{ Na}_2\text{O}\text{-}0.08 \text{ HMBr}_2\text{-}12 \text{ H}_2\text{O}$. At the early crystallization stage (0-6 h), the solid silica species and EU-1-300 seeds dissolved gradually under alkaline aqueous medium and the solution gains the high concentrated nutrition, such as HM and the dissolved EU-1 crystallite precursors. After 6-14 h, XRD patterns are notable for the EU-1 characteristics peaks, this can be explained that the prepared gel composition, especially for high HM content and the addition of EU-1-300 seeds, both benefits for the formation of EU-1 phase.^[19,21] Thereafter, along with an increasing amount of EU-1 phase, and the compositions in both solid and liquid phase are varying simultaneously. More and more nutrition, such as HM ions, EU-1 seeds, especially Al species are consumed and transferred to the solid phase as structure directing agent and/or framework atoms for the formation of EU-1 phase. As decreasing the Al nutrition in the prepared gel, the higher silica mixture gel is suitable for the nucleation of ZSM-48, due to high silica medium and the mixture composition could promote the growth of the ZSM-48 structure phase.^[19] Under this circumstance, thermodynamic stability phase area of the crystallization system tends to adjust the growth balance of each crystal phase in its favour. Due to presence of more high silica EU-1 seeds, EU-1 crystals still can work as effective seeds for subsequent EU-1 growth. As a result, EU-1 and ZSM-48 phases grow competitively (14-20 h), which brings about the co-crystallization of EU-1/ZSM-48 zeolite and a steady crystallization period. More importantly, a phase proportion in the EU-1/ZSM-48 zeolite remains invariable during proceeding 20-36 h crystallization, suggesting the crystallization stability period is as the same with synthesis for an individual zeolite. Thus, this co-growth process is significantly different from the Al-rich EU-1-55 seeds system, where the severe crystal transform from purely high-silica EU-1 zeolite into ZSM-48 phase continued after 24 h.^[21]



Scheme 1. Primary crystallization process of EU-1/ZSM-48 co-crystalline

In this work, no phase transformation of the two phases was found when synthesized at temperature either 433 K or 453 K. The big difference in framework structures and morphologies between EU-1 and ZSM-48 zeolites could result in the microstructure distortion of the EU-1/ZSM-48 co-crystalline zeolite during their competitive growth, giving rise to the special physical-chemical properties, which would exert excellent catalytic performance.

Catalytic performance of EU-1/ZSM-48 co-crystalline zeolites:

The Coz-75, Mix-75, EU-1-300 and ZSM-48-300 are comparatively evaluated in n-hexane catalytic cracking reaction. The catalytic performance of the samples as a function of time on stream displays in Figure 10. The initial n-hexane conversion (TOS=15 min) is in the order of $\text{Coz-75} > \text{EU-1} > \text{Mix-75} > \text{ZSM-48}$, which is extremely in accordance with the order of strong acid amount. Among the four samples, Coz-75 exhibits the highest activity and catalytic stability with time on stream, and the n-hexane conversion over Coz-75 decreases from 93.9 wt% to 80.9 wt% within 600 min. The performance of Mix-75 sample unaffectedly displays in middle of pure EU-1-300 and ZSM-48-300 zeolites.

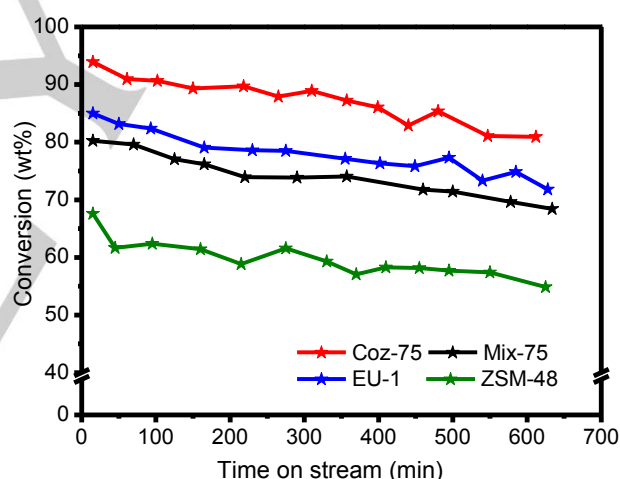


Figure 10. n-Hexane conversion with time on stream over different zeolites

Figure 11 illustrates the initial product yields (TOS=15 min) over different zeolites. Coz-75 displays the highest yields of ethylene (14.7 wt%) and propylene (38.3 wt%), which are respectively higher than Mix-75 by 3.7 and 6.3 percentage points. Noteworthy, the propylene yield over Coz-75 is higher than the single EU-1 zeolite. While previous research reported EU-1 had higher propylene yield than the conventional catalytic cracking catalyst of ZSM-5 by 9.0 percentage points under the same reaction conditions.^[22] During the whole catalytic process, Coz-75 also exhibits the highest yield of the ethylene and propylene than other samples. The yield of ethylene ranges from 14.7 to 11.8 wt% and propylene decreases from 38.3 to 31.9 wt% within 600 min (Figure S6). According to the mechanism of alkane cracking, the alkane molecules initially adsorb on a strong acid sites, especially the strong Brönsted acid sites and form

FULL PAPER

a “carbonium ion type” activated complex, which further accelerates the reaction, leading to a higher initial conversion.^[33] Therefore, Coz-75 with more acid amount and specific texture properties could enhance the control over the cracking products.

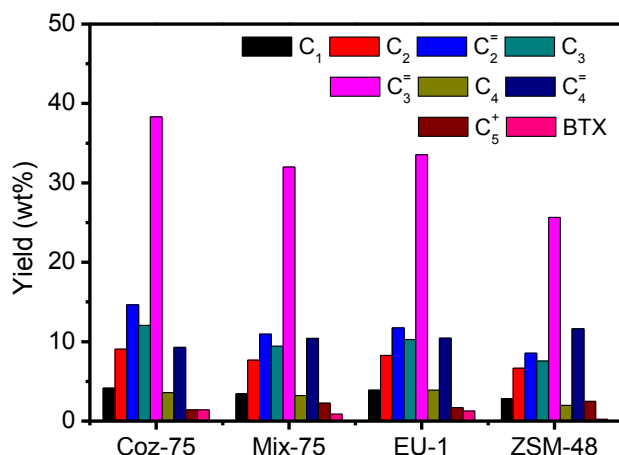


Figure 11. Initial product yield over different zeolites (C₅⁺ stands for the aliphatic hydrocarbons with the carbon number is 5 and higher than 5 except BTX, and BTX stands for benzene, toluene, and xylenes, the same below)

Conclusions

EU-1/ZSM-48 co-crystalline zeolites with various phase proportions were synthesized by seed-assisted approach in the presence of HM. In addition to the HM content and alkalinity, high silica EU-1 seeds (such as SiO₂/Al₂O₃ ratio of 300) is the most crucial factor that generates EU-1 and then ZSM-48 in sequence and controls the crystal proportions of EU-1/ZSM-48 co-crystalline zeolite. With the proportions of EU-1 phase in EU-1/ZSM-48 composite increase from 25 wt% to 86 wt%, the framework SiO₂/Al₂O₃ ratio of EU-1 also increases accordingly. The co-crystallization process of EU-1/ZSM-48 co-crystalline possess a long stability period and no phase transformation occurs at 433 K and 453 K. EU-1/ZSM-48 co-crystalline zeolites with various EU-1 proportions present different texture properties, resulting from the competitive crystallization of the two zeolitic phases, which is ascribed to the notable difference in framework structure and morphology of both phases. The primary crystallization process of EU-1/ZSM-48 co-crystalline zeolites was proposed. In n-hexane catalytic cracking reaction, Coz-75 displays the highest yield of ethylene (14.7 wt%) and propylene (38.3 wt%), which is respectively higher than Mix-75 by 3.7 and 6.3 percentage points. Especially, Coz-75 provides higher propylene yield than the single EU-1 zeolite, while the latter being higher than ZSM-5 by 9.0 percentage points.

Experimental Section

Materials

Hexamethonium bromide (HMBR₂, >98 wt%, A.R.) used as template was purchased from Aldrich. Reagent-grade colloid silica (SiO₂, 40 wt%, Qingdao Haiyang Chemical Co.) was used as silica source. Reagent-grade sodium aluminates

(Al₂O₃, 45 wt%; Na₂O, 27 wt%, A.R.) and sodium hydroxide (NaOH, 99 wt%, A.R.) were purchased from Sinopharm Chemical Reagent Co. All of the reagents were used without further purification.

Synthesis of seed materials

The pure EU-1-300 and ZSM-48-300 were respectively prepared according to the procedure reported in our previous work.^[21] For comparative research, EU-1-300 and ZSM-48-300 as seeds were used in the synthesis of co-crystalline EU-1/ZSM-48. Meanwhile, the mechanical mixture of EU-1-300 and ZSM-48-300 was also investigated as seeds, and was prepared according to the description below.

Synthesis of EU-1/ZSM-48 co-crystalline zeolites

EU-1/ZSM-48 co-crystalline zeolites were hydrothermally synthesized in a seeded system. A series of hydrogels with varying molar compositions SiO₂-1/300Al₂O₃-xNa₂O-yHMBR₂-12H₂O were prepared (x ranged from 0.06 to 0.16, and y ranged from 0.04 to 0.15) by mixing the starting reactants with seeds. The amount of seeds with respect to silica content in the initial gel ranged from 0 to 10 wt%. The final mixture was further stirred and then heated in a Teflon-coated stainless steel autoclave at 433 K or 453 K. After thermal treatment, the reactor was quenched by cooling down the mixture to room temperature. The solid was obtained after filtration, thoroughly wash and then dried at 393 K overnight. The protonated samples were obtained by repeated ion exchange with 1 M NH₄Cl solution for 2 h at 363 K and then calcined at 823 K for 5 h.

A mechanical mixture was prepared by physical mixing of pure EU-1-300 and ZSM-48-300 zeolites in a water bath at 303 K for 2 h with the same weight proportion of EU-1 phase to the EU-1/ZSM-48 co-crystalline zeolites. After filtration, the obtained solid was washed thoroughly with deionized water and then dried at 393 K overnight. The protonated samples of mechanical mixtures were obtained by simply mixing of protonated EU-1 and ZSM-48 zeolites according to the aforesaid method.

The weight proportion of EU-1 phase in EU-1/ZSM-48 co-crystalline zeolites can be deduced from a working curve of the relative diffraction intensities to the EU-1 proportion and the detailed process was described in support information S1.^[5b,13d]

Characterization

Powder X-ray diffraction (XRD) patterns for crystal phase, crystallinity and proportion identification were carried out on a Bruker D8 Advance diffractometer (40 kV, 4 mA) using Cu K α radiation ($\alpha=1.5406 \text{ \AA}$) at a scanning rate of 4 °/min from 5° to 50° (2 θ). The unit cell parameters of EU-1 crystal phase in as-synthesized zeolitic samples were recorded exactly on a Rigaku D/Max 2000 diffractometer (120 kV, 40 mA) with Cu K α radiation ($\alpha=1.5418 \text{ \AA}$) at a scanning rate of 0.5 °/min from 18° to 28° (2 θ).

Fourier transform infrared (FT-IR) spectra were collected by a Nicolet Magna-IR 560 E.S.P instrument using

FULL PAPER

KBr discs in the range of 400-1600 cm^{-1} . The morphologies and the bulk chemical compositions of the obtained samples were derived by Field-emission Environmental Scanning Electron Microscope (SEM, FEI Quanta 200F) and X-ray Fluorescence Analyzer (XRF, PANalytical AxiosMAX), respectively.

Nitrogen adsorption-desorption experiments were measured on a Micromeritics ASAP 2020M instrument at 77 K, and the powder zeolites were evacuated at 823 K for 6 h and degassed at 573 K under vacuum for 5 h. The specific surface area was calculated by Brunauer-Emmett-Teller (BET) equation with the adsorption data obtained at P/P₀ between 0.05 and 0.25. The total pore volume was derived from the nitrogen amount adsorbed at a relative pressure of 0.99. The micropore surface area and volume were calculated by t-plot method. The pore size distribution was determined from the desorption branch of the isotherm according to BJH model.

Temperature-programmed desorption of ammonia (NH₃-TPD) was carried out to evaluate the acidity of the samples on an adsorption instrument (TP-5076, Tianjin Xianquan Industry and Trade Development Co., LTD). Prior to the measurement, the sample (100 mg) was degassed at 873 K for 2 h and then cooled down to 373 K in N₂ flow. After that, the sample was saturated in NH₃-N₂ (mole ratio 1:1) stream for 30 mins, followed by purging with nitrogen for 1 h to remove the physisorbed ammonia. The chemisorbed NH₃ was then determined by heating the sample to 873 K at a constant rate of 10 K/min. The ammonia concentration in the effluent N₂ stream was monitored by thermal conductivity detector (TCD).

²⁹Si Magic Angle Spinning Nuclear Magnetic Resonance (MAS NMR) and ²⁷Al MAS NMR experiments were performed at room temperature on a Varian Infinity-plus 400 MHz spectrometer at a resonance frequency of 79.459 MHz and 104.215 MHz, respectively. ²⁹Si MAS NMR with high power proton decoupling was recorded on a 5 mm probe using a $\pi/4$ single pulse length of 7.2 μs , a recycle delay of 60 s, and a spinning rate of ca.8 kHz. In contrast, ²⁷Al MAS NMR was recorded with a $\pi/4$ single pulse length of 2.1 μs , a recycle delay of 0.5 s, and a spinning rate of 10 kHz on a 4 mm probe. The chemical shifts of ²⁹Si MAS NMR were externally referenced to TMS, whereas that of ²⁷Al MAS NMR was referenced to Al₂(SO₄)₃•12H₂O.

Catalytic measurement

The n-hexane catalytic cracking reaction was performed in a fixed bed reactor under atmospheric pressure. The 0.5 g zeolites were loaded in a quartz tubular reactor (8 mm id) and activated in flowing nitrogen (40 ml•min⁻¹) at 950 K for 1 h. After cooling to 900 K, n-hexane vapor diluted in the nitrogen was fed with the n-hexane partial pressure of 9 kPa and the weight hourly space velocity (WHSV) of n-hexane was 2.0 h⁻¹. The products were analyzed online using an Agilent GC 7890 gas chromatograph equipped with a flame ionization detector (FID) and HP-PLOT Q capillary column (30 m, 0.53 mm id, stationary phase thickness 40 μm). The n-hexane conversion, product selectivity and yields were calculated according to the method in our previous work.^[22]

All of the percent values used in this paper are taken in weight proportions.

Acknowledgements

The authors acknowledge the State Key Development Program for Basic Research of China (2012CB215002), the National Natural Science Foundation of China (21276278, U1662116) and CNPC Key Research Project (2014A-2111) for the financial support of this work.

Keywords: composite zeolite • ZSM-48 • EU-1 • n-hexane • catalytic cracking

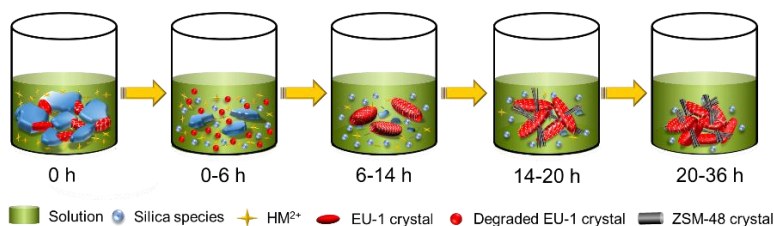
- [1] a) A. Corma, *J. Catal.* **2003**, *216*, 298-312; b) A. Corma, *Chem. Rev.* **1995**, *95*, 559-614; c) R. J. Davis, *J. Catal.* **2003**, *216*, 396-405.
- [2] a) T. Okubo, T. Wakihara, J. Plévert, S. Nair, M. Tsapatsis, Y. Ogawa, H. Komiyama, M. Yoshimura, M. E. Davis, *Angew. Chem. Int. Ed.* **2001**, *40*, 1069-1071; b) Y. Bouizi, L. Rouleau, V. P. Valtchev, *Chem. Mater.* **2006**, *18*, 4959-4966; c) K. Itabashi, Y. Kamimura, K. Iyoki, A. Shimojima, T. Okubo, *J. Am. Chem. Soc.* **2012**, *134*, 11542-11549.
- [3] C. N. R. Rao, J. M. Thomas, *Acc. Chem. Res.* **1985**, *18*, 113-119.
- [4] S. Xie, S. Liu, Y. Liu, X. Li, W. Zhang, L. Xu, *Microporous Mesoporous Mater.* **2009**, *121*, 166-172.
- [5] a) J. M. Thomas, G. R. Millward, *J. Chem. Soc., Chem. Commun.* **1982**, *24*, 1380-1383; b) A. M. Goossens, B. H. Wouters, V. Buschmann, J. A. Martens, *Adv. Mater.* **1999**, *11*, 561-564.
- [6] a) M. S. Francesconi, Z. E. López, D. Uzcátegui, G. González, J. C. Hernández, A. Uzcátegui, A. Loaiza, F. E. Imbert, *Catal. Today* **2005**, *107-108*, 809-815; b) G. A. Jablonski, L. B. Sand, J. A. Gard, *Zeolites* **1986**, *6*, 396-402; c) L. Zhang, S. Liu, S. Xie, L. Xu, *Microporous Mesoporous Mater.* **2012**, *147*, 117-126; d) Y. Song, S. Liu, Q. Wang, L. Xu, Y. Zhai, *Fuel Process. Technol.* **2006**, *87*, 297-302; e) P. Li, W. Zhang, X. Han, X. Bao, *Catal. Lett.* **2009**, *134*, 124-130.
- [7] a) J. B. Higgins, R. B. LaPierre, J. L. Schlenker, A. C. Rohrman, J. D. Wood, G. T. Kerr, W. J. Rohrbach, *Zeolites* **1988**, *8*, 446-452; b) N. Hould, M. Haouas, V. Nikolakis, F. Taulelle, R. Lobo, *Chem. Mater.* **2012**, *24*, 3621-3632.
- [8] L. A. Villaescusa, W. Zhou, R. E. Morris, P. A. Barrett, *J. Mater. Chem.* **2004**, *14*, 1982-1987.
- [9] R. L. Smith, W. A. Stawirski, A. Lind, D. S. Wragg, J. H. Cavka, B. Arstad, H. Fjellvåg, M. P. Atfield, D. Akporiaye, M. W. Anderson, *Chem. Mater.* **2015**, *27*, 4205-4215.
- [10] S. Zanardi, R. Millini, F. Frigerio, A. Belloni, G. Crucia ni, G. Bellussi, A. Carati, C. Rizzo, E. Montanari, *Microporous Mesoporous Mater.* **2011**, *143*, 6-13.
- [11] A. W. Burton, S. I. Zones, T. Rea, I. Y. Chan, *Microporous Mesoporous Mater.* **2010**, *132*, 54-59.
- [12] H. K. Jeong, J. Krohn, K. Sujaoti, M. Tsapatsis, *J. Am. Chem. Soc.* **2002**, *124*, 12966-12968.
- [13] a) X. Niu, Y. Song, S. Xie, S. Liu, Q. Wang, L. Xu, *Catal. Lett.* **2005**, *103*, 211-218; b) X. Qi, D. Kong, X. Yuan, Z. Xu, Y. Wang, J. Zheng, Z. Xie, *J. Mater. Sci.* **2008**, *43*, 5626-5633; c) Y. Fan, D. Lei, G. Shi, X. Bao, *Catal. Today* **2006**, *114*, 388-396; d) X. Zhang, J. Wang, J. Zhong, A. Liu, J. Gao, *Microporous Mesoporous Mater.* **2008**, *108*, 13-21.
- [14] L. Y. Sun, Y. F. Zhang, Y. J. Gong, *Acta Phys-chim Sin* **2016**, *32*, 1105-1122.
- [15] H. Chen, B. Shen, H. Pan, *Chem. Lett.* **2003**, *32*, 726-727.
- [16] G. Zhao, J. Teng, Y. Zhang, Z. Xie, Y. Yue, Q. Chen, Y. Tang, *Appl. Catal., A* **2006**, *299*, 167-174.
- [17] J. Martins, E. Birot, E. Guillon, F. Lemos, F. Ramôa Ribeiro, P. Magnoux, S. Laforge, *Microporous Mesoporous Mater.* **2013**, *171*, 230-237.
- [18] J.L. Casci, T.V. Whittam, US 4537754, **1981**.
- [19] G. Giordano, J. B. Nagy, E. G. Derouane, *J. Mol. Catal. A: Chem.* **2009**, *305*, 34-39.

FULL PAPER

- [20] X. Liu, U. Ravon, A. Tuel, *Microporous Mesoporous Mater.* **2012**, *156*, 257-261.
- [21] Q. Xu, Y. Gong, W. Xu, J. Xu, F. Deng, T. Dou, *J. Colloid Interface Sci.* **2011**, *358*, 252-260.
- [22] Y. F. Zhang, X. L. Liu, L. Y. Sun, Q. H. Xu, X. J. Wang, Y. J. Gong, *Fuel Process. Technol.* **2016**, *153*, 163-172.
- [23] W. Souverijns, L. Rombouts, J. A. Martens, P. A. Jacobs, *Microporous Mater.* **1995**, *4*, 123-130.
- [24] P. C. Mihindou-Koumba, J. D. Comparot, S. Laforge, P. Magnoux, *J. Catal.* **2008**, *255*, 324-334.
- [25] a) R. Szostak, *Molecular Sieves: Principles of Synthesis and Identification*, Springer Netherlands, **1989**, pp 71-95; b) C. S. Cundy, P. A. Cox, *Chem. Rev.* **2003**, *103*, 663-702; c) L. Itani, Y. Liu, W. Zhang, K. N. Bozhilov, L. Delmotte, V. Valtchev, *J. Am. Chem. Soc.* **2009**, *131*, 10127-10139.
- [26] M. Kruk, M. Jaroniec, *Chem. Mater.* **2001**, *13*, 3169-3183.
- [27] J. Zheng, X. Zhang, Y. Zhang, J. Ma, R. Li, *Microporous Mesoporous Mater.* **2009**, *122*, 264-269.
- [28] a) B. Smit, T. L. M. Maesen, *Nature* **2008**, *451*, 671-678; b) M. Caillot, A. Chaumonnot, M. Digne, J. A. van Bokhoven, *J. Catal.* **2014**, *316*, 47-56.
- [29] Z. Yu, A. Zheng, Q. Wang, L. Chen, J. Xu, J.-P. Amoureux, F. Deng, *Angew. Chem. Int. Ed.* **2010**, *49*, 8657-8661.
- [30] A. Arnold, M. Hunger, J. Weitkamp, *Microporous Mesoporous Mater.* **2004**, *67*, 205-213.
- [31] J. Pérez-Pariante, J. Sanz, V. Fornés, A. Corma, *J. Catal.* **1990**, *124*, 217-223.
- [32] G. N. Rao, P. N. Joshi, A. N. Kotasthane, P. Ratnasamy, *Zeolites* **1989**, *9*, 483-490.
- [33] a) A. Corma, A. V. Orchillés, *Microporous Mesoporous Mater.* **2000**, *35-36*, 21-30; b) S. Kotel, H. Knözinger, B. C. Gates, *Microporous Mesoporous Mater.* **2000**, *35-36*, 11-20.

FULL PAPER

FULL PAPER



A series of EU-1/ZSM-48 co-crystalline zeolites with long crystallization stability can be obtained with a high silica seeded method. This article discusses the influences of the different synthesized factors and the synthesis process. The EU-1/ZSM-48 co-crystalline zeolite also displays great performance in n-hexane catalytic cracking reaction.

Yafei Zhang,^[a] Yasheng Liu,^[a] Liyuan Sun,^[a] Luoming Zhang,^[a] Jun Xu,^[b] Feng Deng^[b] and Yanjun Gong,^{*[a]}

Page No. – Page No.

Synthesis of EU-1/ZSM-48 Co-crystalline Zeolite by High Silica EU-1 Seeds: Tailoring Phase Proportions and Promoting Long Crystalline Phase Stability

Accepted Manuscript